Wavelength-independent constant period spin-echo modulated small angle neutron scattering

Sales, Morten; Plomp, Jeroen; Habicht, Klaus; Tremsin, Anton; Bouwman, Wim; Strobl, Markus

DOI
10.1063/1.4954727

Publication date
2016

Document Version
Final published version

Published in
Review of Scientific Instruments

REVIEW OF SCIENTIFIC INSTRUMENTS **87**, 063907 (2016)

Wavelength-independent constant period spin-echo modulated small angle neutron scattering

Morten Sales,[1,a)] Jeroen Plomp,[2] Klaus Habicht,[3] Anton Tremsin,[4] Wim Bouwman,[2] and Markus Strobl[1,5]
[1]*Nano-Science Center, Niels Bohr Institute, University of Copenhagen, DK-2100 Copenhagen, Denmark*
[2]*Faculty of Applied Sciences, Delft University of Technology, 2629 JB Delft, The Netherlands*
[3]*Helmholtz-Zentrum Berlin für Materialen und Energie GmbH, D-14109 Berlin, Germany*
[4]*Space Sciences Laboratory, University of California at Berkeley, Berkeley, California 94720, USA*
[5]*European Spallation Source ESS-AB, Science Division, SE-22100 Lund, Sweden*

(Received 28 December 2015; accepted 11 June 2016; published online 27 June 2016)

Spin-Echo Modulated Small Angle Neutron Scattering (SEMSANS) in Time-of-Flight (ToF) mode has been shown to be a promising technique for measuring (very) small angle neutron scattering (SANS) signals and performing quantitative Dark-Field Imaging (DFI), i.e., SANS with 2D spatial resolution. However, the wavelength dependence of the modulation period in the ToF spin-echo mode has so far limited the useful modulation periods to those resolvable with the limited spatial resolution of the detectors available. Here we present our results of an approach to keep the period of the induced modulation constant for the wavelengths utilised in ToF. This is achieved by ramping the magnetic fields in the coils responsible for creating the spatially modulated beam in synchronisation with the neutron pulse, thus keeping the modulation period constant for all wavelengths. Such a setup enables the decoupling of the spatial detector resolution from the resolution of the modulation period by the use of slits or gratings in analogy to the approach in grating-based neutron DFI. *Published by AIP Publishing.* [http://dx.doi.org/10.1063/1.4954727]

I. INTRODUCTION

Spin-Echo Modulated Small Angle Neutron Scattering (SEMSANS) has been proven to be possible and a useful small angle neutron scattering (SANS) tool for utilising either a monochromatic beam[1] or a pulsed neutron beam,[2,3] just as in conventional SANS.[4] It has also been shown that the method holds the outstanding potential to measure SANS with additional spatial resolution on the macroscopic scale of neutron imaging[5] in analogy to grating based Dark-Field Imaging (DFI).[6]

In general, SEMSANS and in particular SEMSANS-based DFI is highly analogous to the grating interferometer based dark-field method. However, to date, the two methods operate at very different ranges of modulation periods and correspondingly also scattering vector and resolvable size ranges. For monochromatic SEMSANS, just as for grating interferometry, the period of the spatial beam modulation during an exposure is constant. This allows for analysis of the modulation utilising a phase-stepping, i.e., scanning, approach with an absorption grating matching the period of the modulation in front of the detector.[7] Either the modulation or the analyser grating is shifted across the beam and a number of images are recorded over one period. This in turn enables periods to be resolved which are smaller than the detector resolution, in the same way as Dark-Field Imaging (DFI) with grating interferometers. In SEMSANS, the periods are currently also limited by the magnetic field setups, but in particular in the Time-of-Flight (ToF) realisation, the spatial detector resolution constitutes the main limitation.

For SEMSANS, a polarised neutron beam is laterally modulated in the detector plane by modulating the polarisation with two triangular field regions[3,8–10] with fields in opposite directions. The modulated polarisation across the beam is turned into an intensity modulation by the use of a polarisation analyser.

Downstream from the analyser at the detector position, the now spatial modulation has a period given by[8]

$$\zeta = \frac{\pi \tan\theta_0}{c\lambda\,(B_2 - B_1)}, \tag{1}$$

with B_1 and B_2 being the fields in the triangular coils, θ_0 the inclination angle of the triangular coils with respect to the optical axis, the Larmor constant $c = 4.632 \times 10^{14}$ T^{-1} m^{-2}, and λ the wavelength. It can be seen that for a constant angle, θ_0, and fields, B_1 and B_2, in the triangular coils, the period will decrease with increasing wavelength. Hence, throughout a neutron pulse in a ToF instrument, where neutrons with higher energy (velocity) and hence shorter wavelengths arrive at the detector first, the modulation period is becoming inversely smaller proportional to the specific ToF of a neutron. The time, t, it takes for a neutron to travel the distance, L (from pulse generating choppers to detector), is, using the de-Broglie equation, given by $t_{TOF} = \alpha L\lambda$, where $\alpha = m_N/h = 2.528 \times 10^{-4}$ s/m/Å, and m_N is the neutron mass and h is the Planck constant.

a)Electronic mail: lsp260@alumni.ku.dk

As the length scale probed, which is characterised by the spin-echo length, δ^{SE}, is given by

$$\delta^{SE} = \frac{\lambda L_S}{\zeta} = \frac{c\lambda^2 L_S(B_2 - B_1)}{\pi \tan\theta_0}, \tag{2}$$

where L_S is the distance from sample to detector, the probed scale is proportional to the wavelength, and hence also ToF, squared. This is the case because both the period, which defines the scattering angle probed, and the scattering angles, which relate to the scattering structure sizes, are linearly wavelength dependent.

In SEMSANS, the magnetic fields in the two triangular precession regions and their distances to the detector have to fulfil the focusing condition $B_1L_1 = B_2L_2$ (where L_1 (L_2) is the distance from the first (second) triangular coil to the detector) in order to achieve an optimised modulation in the detector plane. This condition is wavelength independent, and hence the method can be exploited efficiently in ToF mode. In contrast to this, a neutron grating interferometry setup is optimised to a specific wavelength, because of the wavelength dependency of the fractional Talbot distance as well as the induced phase shift in the phase gratings.[7,11] Therefore, although it has been shown that contrast can still be achieved over a range of a few angstroms,[12] the grating interferometry setup is generally not well suited for ToF applications, in particular with respect to a significant range to be probed efficiently.

When considering how to keep the modulation period constant in a ToF SEMSANS experiment, either the magnetic field in the precession coils or their angular setup has to be adapted in synchronisation with the ToF pulses. Given the frequencies of about 10 Hz to 50 Hz in most neutron ToF applications and the potential to adapt and synchronise the magnetic fields remotely by the supplied electrical currents, such an option was chosen over a mechanical adaptation of the angles of the field regions. In order to keep the modulation period constant, the required field values for B_1 and B_2 can easily be calculated by

$$B_1(t_1) = B_2(t_2)\frac{L_2}{L_1} = \frac{1}{\lambda}\frac{\pi \tan\theta_0 L_2}{c\zeta(L_1 - L_2)}, \tag{3}$$

$$B_1(t) = \frac{\alpha(L - L_1)}{t}\frac{\pi \tan\theta_0 L_2}{c\zeta(L_1 - L_2)}, \tag{4}$$

$$B_2(t) = \frac{\alpha(L - L_2)}{t}\frac{\pi \tan\theta_0 L_2}{c\zeta(L_1 - L_2)}, \tag{5}$$

where t_1 (t_2) is the arrival time of a neutron at the first (second) triangular coil.

The practical differences in the ramped and constant field method are illustrated in Fig. 1. With the ramped field, a linear dependence of the spin-echo length on the wavelength is obtained, instead of the square one as the constant field method yields (see Fig. 1(b)).

The range in spin-echo length is therefore smaller in the ramped case than in the constant field method. The lower limit in spin-echo length is determined by the maximum field that is achievable in the triangular coils, the upper limit by the detector resolution.

II. MEASUREMENTS

The measurements were performed at the Reactor Institute Delft, TUDelft, The Netherlands. The pulsed beam was created using a co-rotating optically blind double chopper setup,[13] with about 5% $\delta\lambda/\lambda$ at the detector and a pulse frequency of 50 Hz. The neutrons were polarised and analysed using multi-channel supermirrors, and the neutron spin-rotations were controlled using V-coils (Delft $\pi/2$-rotators[14]). The current in the triangular coils was controlled with a pulse generator for each coil with a peak magnetic field of about 3 mT. The data were recorded using a microchannel plate detector with a pixel size of 55×55 μm^2 and timepix readout[15,16] with time frame exposure of 48 μs (rebinned into 96 μs).

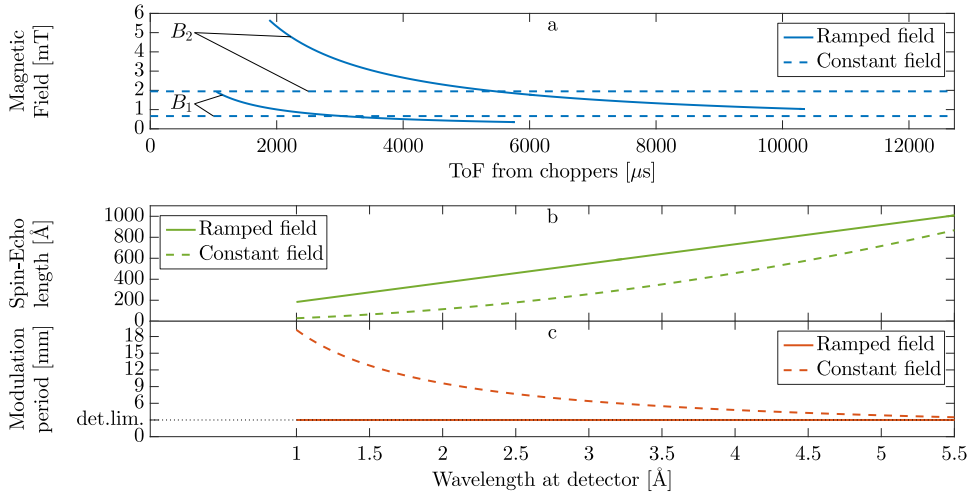

FIG. 1. Calculated example curves. (a) ToF dependence of magnetic fields in ramped field setup. To keep the modulation period wavelength independent, the magnetic field in the triangular coils must be stronger for faster neutrons (see Eq. (1)). Curves for constant fields setup shown for comparison. ((b) and (c)) Spin-echo length, δ^{SE}, and modulation period, ζ, as a function of wavelength for ramped and constant field setups. The limit of a detector being able to resolve a minimum modulation period of 3 mm is marked in (c) ($L_S = 0.55$ m, $L_1 = 5.0$ m, $L_2 = 1.7$ m, $L = 9.15$ m, $\theta_0 = 20°$).

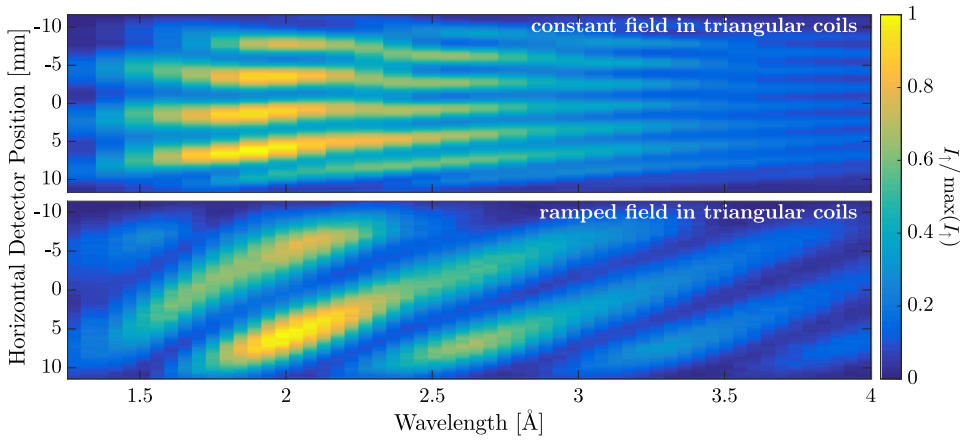

FIG. 2. Spin-echo induced spatial modulation without and with neutron pulse synchronised ramped magnetic fields in triangular coils. (Multimedia view) [URL: http://dx.doi.org/10.1063/1.4954727.1]

Measurements with constant magnetic fields in the triangular coils, and therefore wavelength dependent modulation period, were recorded as well for comparison.

III. RESULTS

Fig. 2 (Multimedia view) shows the measurements of the spatial modulation with and without ramped fields as a function of wavelength. It can be seen that with constant magnetic field in the triangular precession coils, the modulation period decreases with increasing wavelength. When the magnetic fields are ramped, the period could be stabilised but still small changes are observed with the current setup. Furthermore, it can be seen that when ramping the magnetic fields, the modulation pattern shifts across the detector surface, since the magnetic field strengths scale with the distance from coil to detector and therefore the spin-echo position is being moved horizontally across the detector surface during the neutron pulse. This means that in order to keep the modulation stationary as well as with a constant period, a third ramped precession field without inclined field surface is necessary to compensate for the difference in field strength between B_1 and B_2.

In Figs. 3(a)–3(c), examples of the modulation pattern for three different wavelength are shown for both the ramped field and the constant field setup. It can be seen that we succeeded in reducing the wavelength dependence of the modulation period significantly (see also Fig. 2 (Multimedia view)). As further illustrated by Fig. 4, where the modulation period is shown as a function of wavelength, the period is kept constant first in a range where field differences are large, but accuracy in synchronisation between ramped fields and neutron pulse was not sufficient for longer wavelengths (above ~1.6 Å), where the sensitivity of period versus field value increases. This, however, is a simple limitation of the available equipment in our proof-of-principle setup. With appropriate equipment, the

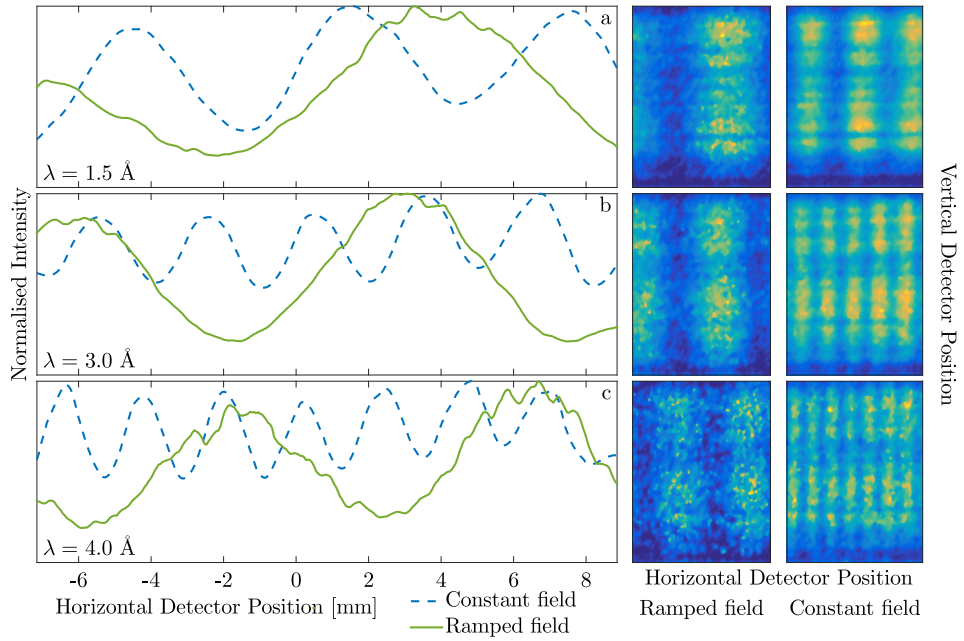

FIG. 3. (a)–(c) show examples of modulation curves for three different wavelengths, with the corresponding detector images on the right.

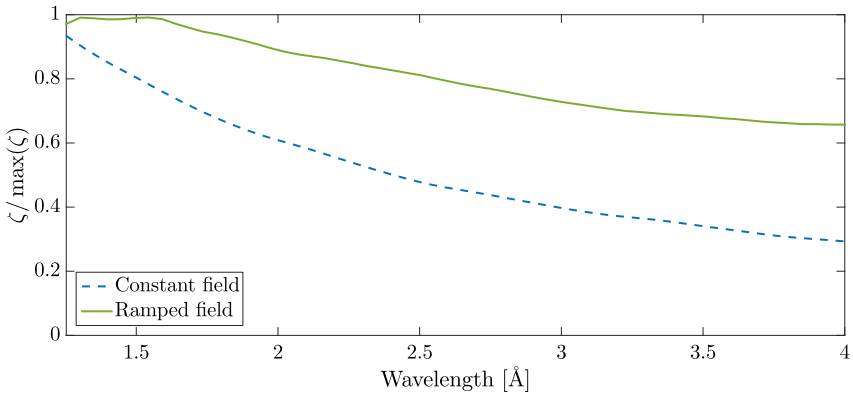

FIG. 4. Comparison of the modulation period as a function of wavelength for constant and for ramped fields in the triangular coils.

synchronisation of the magnetic fields with the neutron pulse and their accuracy will not be limited by the response of the power supply when the induction in the coils are taken into account carefully.

IV. CONCLUSION

We have successfully demonstrated with our proof-of-principle instrumental setup that ramping the magnetic field in the triangular coils of a ToF SEMSANS instrument in synchronisation with ToF neutron pulses makes it possible to keep the spatial modulation period constant during the experiment independent of the ToF and neutron wavelength. This opens up the possibilities for performing quantitative dark field imaging in ToF mode and using a grating analyser to resolve periods beyond the resolution of the detector. This will enable to extend the structure size range amenable by Spin-Echo Modulated Dark Field Imaging (SEM-DFI) as well as in measuring (very) small angle scattering signals with relaxed collimation and a single pixel detector behind a grating also in ToF mode.

Our technique (possibly combined with SANS for investigations of simultaneous structural changes on an even broader length scale range) makes it possible to investigate chemical processes and growth of hierarchical structures, as well as samples such as precipitates in steel or samples in a magnetic environment such as the magnetic field from an electric motor in a rheometer.

The disadvantage of our approach is as demonstrated the limitation in the spin-echo range compared to the constant field setup. However, this is more than balanced by an extended wavelength and period range amenable with this technique using a grating analyser in ToF.

[1]M. Strobl, F. Wieder, C. Duif, A. Hilger, N. Kardjilov, I. Manke, and W. Bouwman, Phys. B **407**, 4132 (2012).
[2]M. Strobl, A. S. Tremsin, A. Hilger, F. Wieder, N. Kardjilov, I. Manke, W. G. Bouwman, and J. Plomp, J. Appl. Phys. **112**, 014503 (2012).
[3]M. Sales, J. Plomp, K. Habicht, and M. Strobl, J. Appl. Crystallogr. **48**, 92 (2015).
[4]D. I. Svergun and L. A. Feigin, in *Structure Analysis by Small-Angle X-Ray and Neutron Scattering*, edited by G. W. Taylor (Plenum Press, 1987).
[5]M. Strobl, M. Sales, J. Plomp, W. G. Bouwman, A. S. Tremsin, A. Kaestner, C. Pappas, and K. Habicht, Sci. Rep. **5**, 16576 (2015).
[6]M. Strobl, Sci. Rep. **4**, 7243 (2014).
[7]F. Pfeiffer, C. Grünzweig, O. Bunk, G. Frei, E. Lehmann, and C. David, Phys. Rev. Lett. **96**, 215505 (2006).
[8]R. Gähler, Phys. B **397**, 1 (2007).
[9]W. G. Bouwman, C. P. Duif, and R. Gähler, Phys. B **404**, 2585 (2009).
[10]W. G. Bouwman, C. P. Duif, J. Plomp, A. Wiedenmann, and R. Gähler, Phys. B **406**, 2357 (2011).
[11]T. Weitkamp, A. Diaz, C. David, F. Pfeiffer, M. Stampanoni, P. Cloetens, and E. Ziegler, Opt. Express **13**, 6296 (2005).
[12]I. Manke, N. Kardjilov, R. Schäfer, A. Hilger, M. Strobl, M. Dawson, C. Grünzweig, G. Behr, M. Hentschel, C. David, A. Kupsch, A. Lange, and J. Banhart, Nat. Commun. **1**, 125 (2010).
[13]A. van Well, Phys. B **180-181**, 959 (1992).
[14]W. Kraan, S. Grigoriev, M. Rekveldt, H. Fredrikze, C. de Vroege, and J. Plomp, Nucl. Instrum. Methods Phys. Res., Sect. A **510**, 334 (2003).
[15]A. S. Tremsin, Neutron News **23**, 35 (2012).
[16]A. Tremsin, J. Vallerga, J. McPhate, and O. Siegmund, Nucl. Instrum. Methods Phys. Res., Sect. A **787**, 20 (2015).